Analysis of a Passive Flow Control Device via Flow Visualization Techniques

Cheryl Graham[1] and Peter Huang.[2]
California Polytechnic State University, San Luis Obispo, CA, 93405

This report details an experiment done to verify the effectiveness of a passive flow control system on a two-dimensional bluff body, blunt trailing edge model in controlling wake dimension and Karman vortex sheds. An earlier experiment by Park, et.al.[1] performed analysis via wind tunnel pressure testing and computerized model to determine the ideal proportions of such a tab design and identify the flow properties responsible for the potential drag reduction. To obtain visual verification of the existence of these concepts, a bluff body model proportionally identical to the one used by Park, et.al., was designed and tested in a water tunnel. The model incorporated a distribution system to dispense the colored dye that allowed visualization of the Karman vortices and related flow characteristics. Two endplates, one with the passive control system and one without, were each tested on the bluff body. Comparison of images captured from the two tests revealed the tab system induced flow characteristics indicative of 3D forcing and drag reduction. Additional investigation of the system performed by varying the angle of attack revealed a decrease in the tab device's effectiveness as angle to the flow increased. Further experimentation could be done to investigate if modifications exist to improve the performance of the system in conditions not parallel to freestream flow; such a system would expand the potential applications of this passive flow control device in aerodynamic applications.

Nomenclature

b	=	span
h	=	vertical depth of bluff body, z axis
y	=	streamwise axis
Re	=	Reynold's number, $(\rho_\infty V_\infty c)/\mu$
z	=	spanwise axis
α	=	angle of attack

I. Introduction

THE experiment herein delineated attempts to verify through flow visualization the computer simulation and wind tunnel pressure findings from a study by Park et.al which claim a tab passive control system successfully decreases vortex shed effects on a two-dimensional bluff body, blunt trailing edge shape. A "bluff body" refers to a shape with a broad, flattened front; a "blunt trailing edge" refers to an end surface perpendicular to the body, appearing immediately at the body's end - no gradual sloping. Examples of bluff body, blunt trailing edge conditions include flows past aircraft, re-entry vehicles, cars, submarines, missiles, and bridge structures. The numerous occurrences of this shape in engineering applications provide motivation and rationale for researching methods to control flow and reduce drag over such bodies.

[1] Undergraduate Student, Aerospace Engineering Department, California Polytechnic State University, San Luis Obispo, 93405.
[2] Undergraduate Student, Aerospace Engineering Department, California Polytechnic State University, San Luis Obispo, 93405.

B. Previous Studies

Drag reduction and flow control requires an understanding of the aerodynamics and fluid behaviors occurring around and behind a bluff body. At critical Reynolds number dependent upon the body shape, the flow separates behind the body and forms two stable and distinct vortices that remain in a fixed position. However, as Reynolds number continues to increase, the flow behind the body becomes unstable and the vortices, instead of remaining fixed, are shed from the body and flow downstream, a phenomenon called Karman vortex shedding. Increased Reynolds numbers cause a distinct wake to form behind the body containing the vortices[2]. Karman vortexes produce a significant pressure drop behind the body, possibly inducing a number of undesirable effects including an increase in mean drag and lift fluctuations. If these vortex phenomena could be controlled by some passive or active control system, their effects could be minimized or their locations altered to produce favorable conditions instead of drag increases[3].

Many past studies examining control methods for flow over bluff bodies have been performed. Choi, Jeon, and Kim[3] provide an excellent overview and analysis of passive and active control systems under consideration or previously seen. In recent years, focus has been on altering the vortex shedding and near wake flow to possibly use them to advantage instead of attempting to remove them entirely. Because active control systems potentially require power inputs and feedback sensors, recent research has focused on less complex passive methods requiring no sensing or actuation. Among these systems, spanwise modifications of the trailing edge have been proven most effective in reducing drag on a 2D body; consequently, much attention from researchers has been directed toward identifying the means by which spanwise modification affects flow, and what passive models would then work best in drag reduction. Choi, et.al. refers to the main effect of spanwise modifications as "3D forcing", which more directly describes the reason such methods affect drag and Karman vortex formation: they force the two dimensional wake structure into a three dimensional one by some variation of geometry along the body or on the trailing edge.

A detailed analysis of one such passive control device on a bluff body, blunt trailing edge two-dimensional shape was performed by Park, Lee, Jeon et.al.[1] In the report introduction Park describes how suppressing the Karman vortex shedding into a steady and symmetric structure reduces their negative effects. The experiment investigated the flow characteristics exhibited by several passive device designs which used tabular modifications to the trailing edge to perturb the wake and induce three dimensional flow. Testing several variations of the tabular ridge, the study found through both wind tunnel testing and computer simulation that a tab system did indeed control the Karman vortex shedding and minimize accompanying pressure effects. It was concluded that the tabs effectively disturbed the vortex shedding from the upper and lower trailing edges to induce spanwise phase mismatch[3]. Karman vortex sheds disappeared directly behind the body and reappeared farther downstream with much less strength than vortices seen on uncontrolled bluff bodies, and several other unique flow changes were identified as indicators of spanwise mismatch. The study also determined that the optimum passive control system design placed three tabs on top and three on bottom, symmetrically, of the trailing edge, with dimensions dependent on the vertical thickness of the bluff body.

D. Objectives

This report describes an experiment designed to corroborate the claims made in Park, et.al. that the described passive control device decreases drag by method of 3D forcing, using a flow visualization test of a similar bluff body model in a water tunnel. Specifically, this study intends to demonstrate that the tab system produces the flow conditions indicative of 3D forcing described by Park, et.al.: a reduced wake width, increased vortex formation length, steady and symmetric vortex formation, and an increased difference from the trailing edge of the bluff body to the beginning of vortex formation. The experiment will require design and manufacturing of a proportionally similar bluff body, blunt nose model and visualization testing in a water tunnel. By incorporating a dye distribution system into the internal structure of the model, colored dye will be released through tiny ports in the trailing edge directly beside the tabs to mark the Karman vortex formation induced by the tab and thus provide visual affirmation that the drag-reducing flow conditions occur. The model will also be tested without the passive system to provide a comparison control case. To further investigate the potential of this passive device, both models will be tested at an angle of attack of 10 , then at increasing increments to observe if the control system remains effective at angles not parallel to freestream flow.

II. Model Design Analysis

In order to acquire data acceptable for use verifying the results of the wind tunnel and simulation experiment, it was essential that the blunt nose, bluff body model constructed for the flow visualization demonstration be dimensionally proportionate and similar in laminar surface properties to that used in the wind tunnel.

A. Conceptual Design Process

Park's experiment analyzed various dimensions and setups of the tabular control system, and determined the optimum tab design and dimensions as depicted in Fig. 1 below.

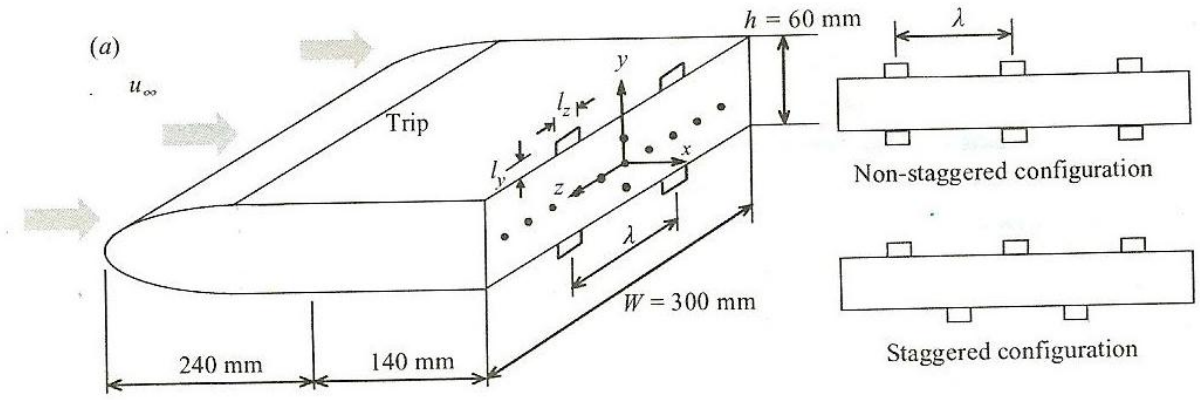

Figure 1. The model used by Park, et.al is shown here. The model used for the flow visualization study used the same shape with dimensions proportionally modified for a different test section size, and the non-staggered tab configuration.

This was used as the basis for designing the flow visualization model. Park specified the bluff body's dimensions in terms of the spanwise width, length parallel to the freestream flow, and model thickness. These directions are defined as x, y, and z respectively. The dimensions of the water tunnel model had to be altered due to the smaller test section size in the water tunnel. The spanwise width of the water tunnel was identified as the driving dimension; the model must touch the edges of the tunnel, to provide a two-dimensional profile, when connected to mounting plates employed to position the model in the test section. This measured out to 6.33''. Using the ratio of this spanwise width to that of the wind tunnel model as a proportional constant, the required vertical depth, streamwise length, and major axis of the elliptic blunt nose of the water tunnel model were also calculated. .

The wind tunnel and simulation results determined that a spanwise array of three tabs symmetrically placed along the top and bottom of the trailing edge of the bluff body offered the optimum passive control system design. The y and z dimensions of the optimum tab size were also determined and presented as a function of the vertical depth of the bluff body. Manufacturing constraints held the minimum x dimension at 1mm, or .039''. Park determined optimum y and z dimensions as .067*h and .2*h, respectively. These formulas produced tabs on the flow visualization model of dimensions (x,y,z) = (.0394, .0848, .2532) inches. The spacing between the tabs was determined by similar relations.

B. Manufacturing

With a preliminary sketch complete and dimensions determined, manufacturing procedures now needed consideration. The reduced model size would require precision in construction, particularly the minute dimensions of the tabs, the most important component of the model. Several members of the Cal Poly Industrial and Manufacturing Engineering Department consented to assist here. Review of the preliminary drawings proved the base design a feasible, but the necessary inbuilt dye distribution system introduced manufacturing complications. The system would require very small outlets on the trailing edge, to let out enough dye to color the flow but not at too high a velocity or volume that it might disturb the flow. The outlets needed to be located as close as possible to the tabs to ensure visualization of the flow characteristics the tabs induced. Consulting again with the IME department, it was decided that the dye system would affect the overall manufacturing process of the bluff body model. Several construction options for the model were considered: making the body, tab end plate, and dye distribution system as separate pieces; making all one part; and making the body and tab end plate separate with

parts of the distribution system incorporated into each. The three-part model was rejected due to concerns that joints between pieces, if not perfectly aligned, would disrupt the laminar flow over the model; less joints was preferable. To negate these aerodynamic reasons, the second option then seemed best, but consultation with manufacturing determined the system too complex and the channels needed too small for rapid prototyping to accurately form inside the model while being built. Thus the third option was chosen. The body – nose and all the streamwise length minus a half centimeter – would be made as one piece. Another piece, the half centimeter length used here, would contain channels on the back side to carry dye to holes placed directly beside the tabs. One channel and top and another on the bottom would hopefully prevent gravitational complications in distribution dye to the upper holes.

A completed model allowed for selection of a manufacturing process. Rapid prototyping was chosen due to its precision, relatively low cost, simplicity of tooling, and availability. The rapid prototyping process receives the virtual design from a CAD program and transforms it into layered crossections. The machine takes this information and builds each layer by laying down a mixture of liquid and powder to create the shape directed. The accuracy of the computers involved made it ideal for constructing to tab end piece. Any aberration in the tab dimensions could affect the flow behavior and threaten the validity of the experiment. The tab end plate would include the dye channels in the rapid prototyping design, but the dye outlets would be drilled afterwards; the hole size required was small enough that the material used to build the layers in rapid prototyping might ooze together. The rapid prototyping process was also chosen for the main bluff body, for ease in constructing the elliptical blunt nose without risking the symmetry required. The required tunnels for the dye would be drilled afterwards, since tunnels in general are difficult for rapid prototyping.

While this close attention manufacturing precision was necessary for the requirements of the tab end plate and elliptical nose, the control end plate, with no tabs, did not require such detail. To lower manufacturing costs, balsa wood would be used to construct it.

Over several months, working with the Cal Poly Aerospace Engineering Department lab technician, all parts were completed and drilled. The lengthy time taken to complete the process was due to an unfamiliarity with the tools and materials, and thus a need for the lab technician and experimenters to research and practice with the tools and materials..

III. Instrumentation and Procedure

The experiment used Cal Poly's water tunnel, an Eidetics' Flow Visualization Water Tunnel with model number 0710 S/N 0025 produced by Rolling Hills Research Company. Fig. 2 shows the three-view schematics of the water tunnel.

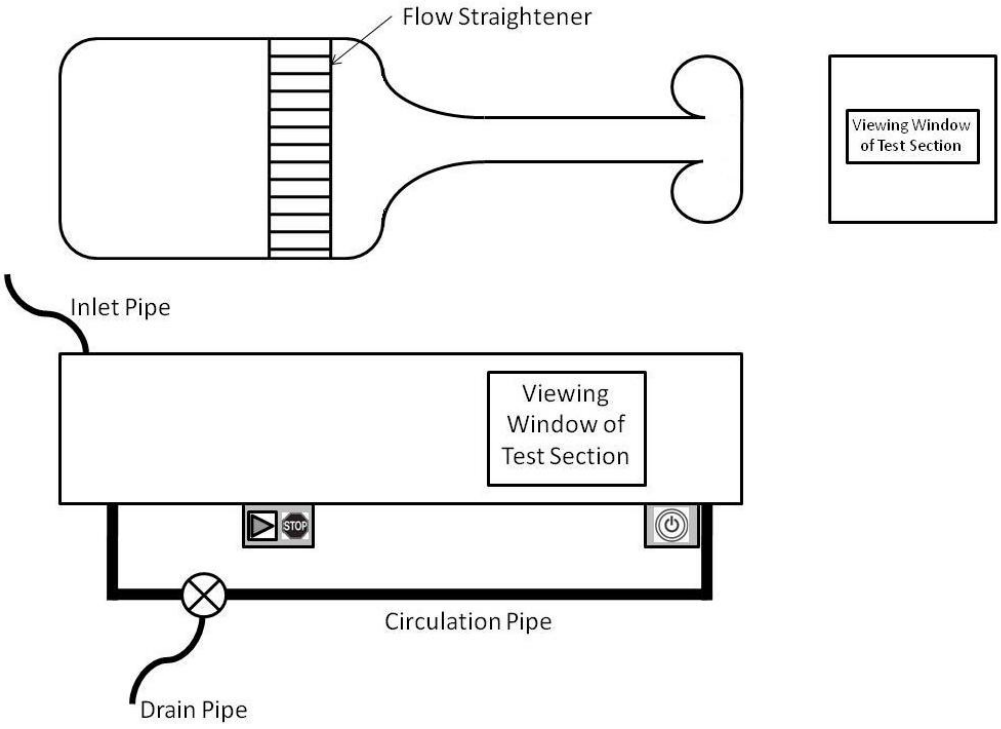

Figure 2. The top, back, and side views of the water tunnel are shown here.

The water tunnel's test-section measured 0.44 m by 0.25 m by 0.19 m with glass viewing windows on the sides. A flow straightener positioned upstream of the test section ensured water flow impinged directly onto the model and not at angles that may have caused irregular turbulence. An outlet pipe allowed for draining of the tunnel. Flow speed is controlled via a variable free stream velocity control mechanism capable of propelling the flow free stream velocity from 0 m/s to about 0.8 m/s.

A. Model Instrumentation

The water tunnel has no top cover, leaving the upper layers of water potentially susceptible to atmospheric disturbances. Avoiding any potential disturbances from ambient conditions or surface flow behavior necessitated filling the water tunnel approximately 90% of full capacity to ensure the model had sufficient depth to prevent disturbances from the upper layers.

Before placing the bluff body model in the tunnel, the dye distribution system needed connecting. In order to precisely control the amount of dye released into the water tunnel, two manual-control dye pressurization systems are used. The original mechanism in the lab for dye release consisted of a rubber chamber filled with dye and hung several feet above the tunnel to provide a gradient that would move the dye through connecting plastic tubes. Unfortunately this system failed to move dye through the PVC tubes used in the model's; it is hypothesized that some interaction between the dye and internal tube material, which differed from the bag's tubes, prevented the flow from continuing into the model. To solve this problem a pressurized system was created out of 10-cc plastic syringes, connected to the model via PVC tubing fitted into the drilled holes in the model body. Waterproof sealant was used to reinforce the connection between the PVC tubing and the plastic syringe. Fig. 3 depicts the new dye control device.

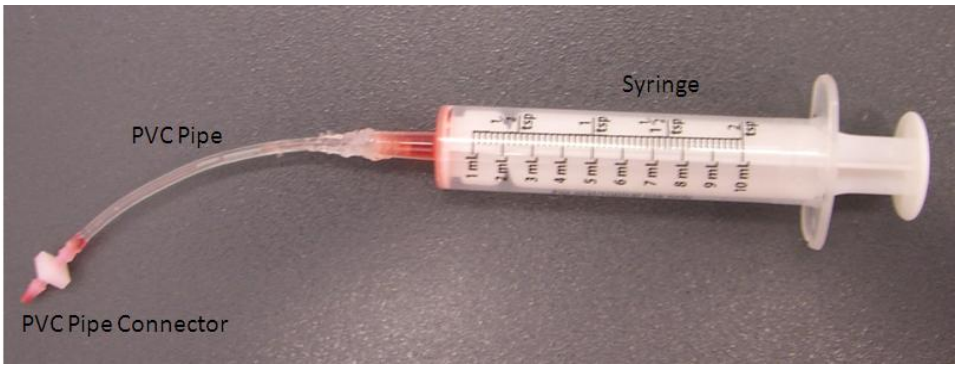

Figure 3. A syringe filled with dye and connected by PVC tubes to channels in the model provided control of dye flow.

Filled with dye, pressure on the syringe's plunging mechanism would move dye into the model and out the dye portals drilled in the attached endplates. Two syringes were used; one to control the top dye outlets and the other the bottom outlets. When all dye outlets were connected to a single pressurization system, the near-edge bottom outlets would release far more dye than the top and far edges, and the pressure required to move dye to the top holes would cause high speed dye released from the bottom holes, affecting the flow and negating the validity of the experiment. Additionally, too much dye released at an instant would decrease the visibility of the water tunnel and create difficulties picking out any vortex disturbances from the rest of the flow.

To fit the model into the water tunnel's mounting system, two sheets of Plexiglass, with a thickness of 3 mm, were glued to each side of the bluff body as seen in Fig 4.

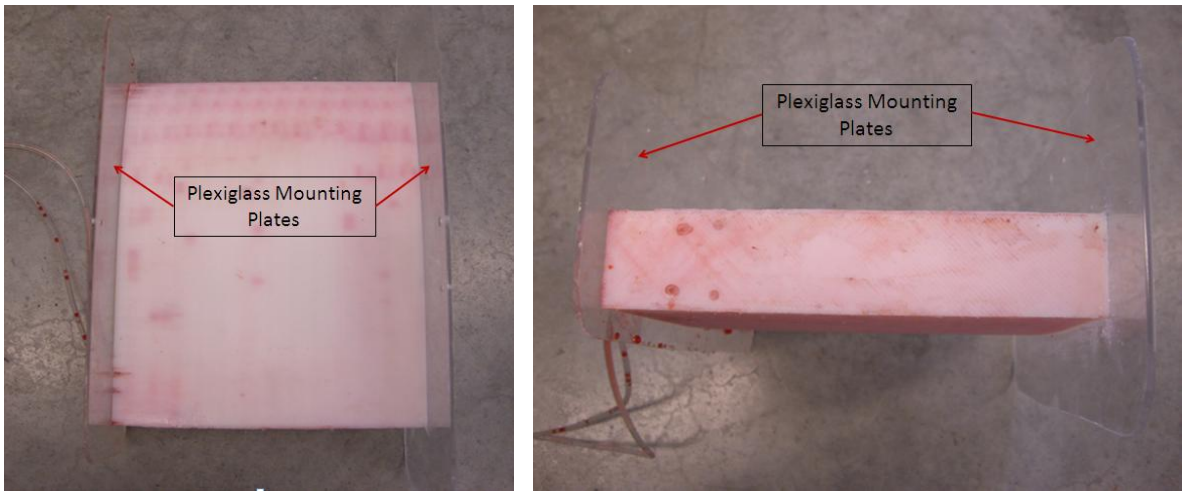

Figure 4. Here the model is shown attached to mounting plates that gave the body a two-dimensional nature to the flow.

The mounting plates would induce two dimensional flow over the bluff body, and allow connection of the model to a mounting fixture on the water tunnel, shown in Fig. 5, constructed by previous researcher(s).

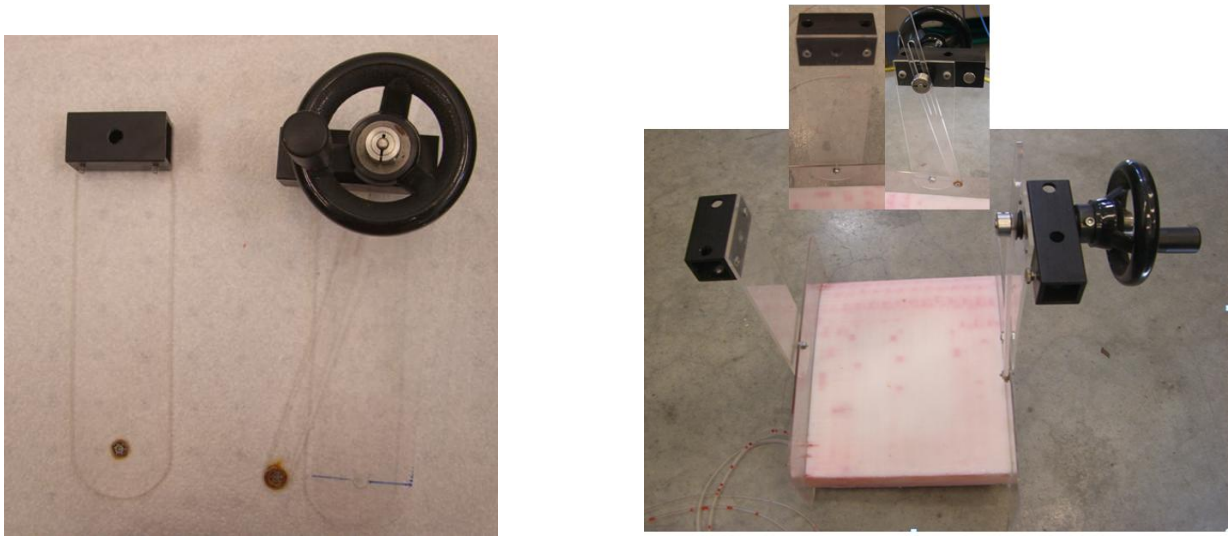

Figure 5. A fixture of Plexiglass and connecting screws was in use to hold models in the water tunnel.

In order to properly connect the tunnel mounting fixture with the Plexiglass mounting plates shown in Figure XX, two sets of #4-40 x 3/8" nuts and screws and one set of #10-32 x 3/8" nut and screw are used. Figure XX shows the proper connections between the mounting mechanism and Plexiglass mounting plates.

To lower manufacturing cost of the model balsa wood was used to construct the control case endplate (without tabs) as shown in Fig. 6.

Figure 6. This wooden end plate was attached to the blunt trailing edge during the control test.

The wood end plate has dimension 162 mm by 34 mm by 6.7 mm and two separate dye channels with three dye outlets in each channel. Fig. 6 shows the wood end plate after using red dye in the experiment. The balsa wood fiber's property of expanding after absorbing liquid unfortunately presented difficulties after repeated use. The end plate expanded in all three dimensions and the dye outlets shrank in diameter. Fortunately, this phenomenon was not severe enough to have any noticeably significant effect on the visualization result, and did not occur until late into the experiment.

B. Experimental Procedure

The flow visualization experiment was split into two separate tests: visualization with the tabs and without the tabs. The experimental apparatus set-up procedure remains the same for both tests.

Due to timing of the end plate construction, the tab case was tested first In order to expedite the set up process, the water inlet pipe was turned on to fill the water tunnel after ensuring the drain pipe was tightly shut. The water tunnel required about 15 to 20 minutes to fill to about 90% capacity; it should never be filled up to over 95% capacity, as water may spill over when model is being submerged. Final assembly of the model and end plate was now done using waterproof sealant to glue the end plate and the bluff body together. Any extra sealant remaining near the dye channels and outlets was wiped away to prevent clogging, and the pieces allowed to dry for 15 minutes. Once dry, the side mounting plates of the model were connected to the mounting apparatus installed on the water tunnel as depicted in Fig. 6 earlier. When the water tunnel reached 90% capacity, the water inlet pipe was shut off, and the bluff body is submerged into the water tunnel's test section as shown in Fig. 7 and secured with hexagonal screws.

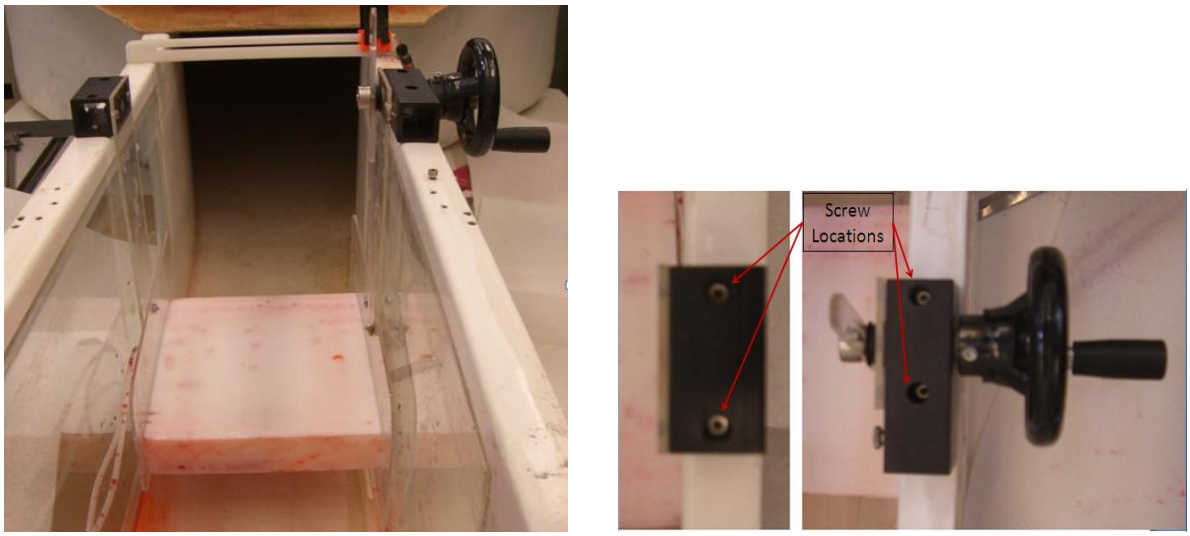

Figure 7. The tunnel mounting fixture held the model in place, and connected to the test section via tightened screws.

The dye pressurization systems were next filled with red food dye. Food dye must be fresh, because as discovered during the failure of the original dye container, old or oxidized food dye tends to form condensed jelly-like substance that could clog the dye channels and outlets. The dye pressurization systems was then connected with the PVC dye inlet tubing from the bluff body as shown in Fig. 8 below.

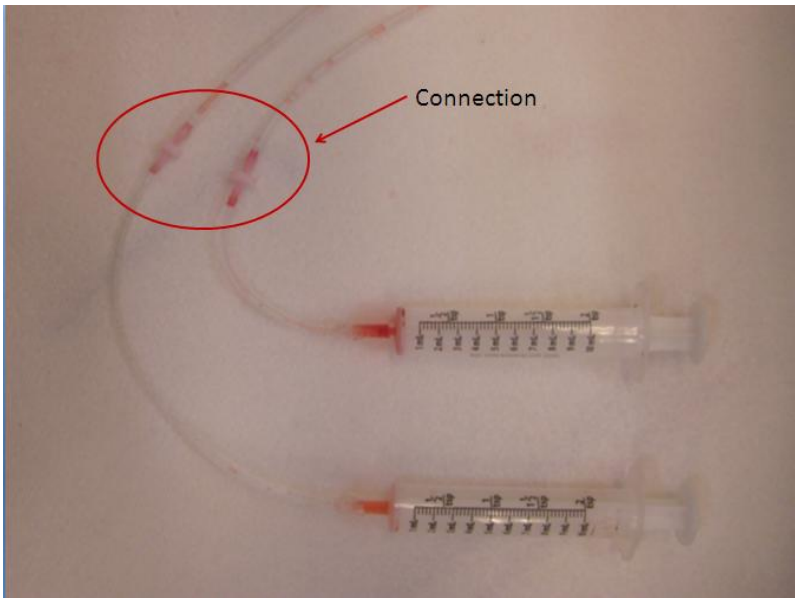

Figure 8. The model's built-in dye tubes were connected to the pressurization system via PVC tubing.

A rotational control rod controlled the angle of the model to a zero degree orientation with respect to the free stream. It was set to 0 for the first test. Fig. 9 shows the location of the rotational control rod.

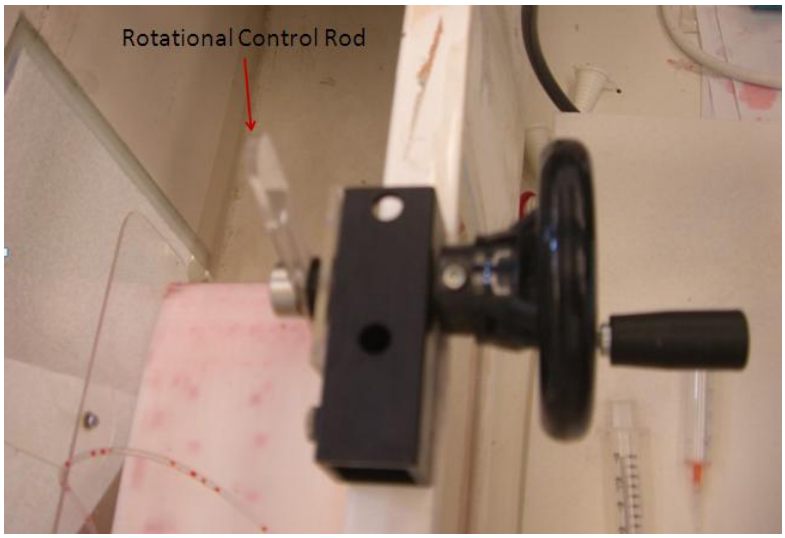

Figure 9. This rotational control rod controlled the orientation of the model with respect to freestream flow.

With all components in place, the water tunnel was turned on and its free stream speed set close to its maximum speed. Running the water tunnel at maximum speed over a long duration of time unnecessarily wears the system quickly. One experimenter stood to the side to capture images while the other controlled the dye flow. Due to the high viscosity of the food dye, a continuous manual press on the syringe's pressure tab was not necessary; instead of continuous press, a slight tap on the pressure tab at regular interval distributed an ideal amount of dye – not too much to overwhelm the test area and not too quickly to chance disturbing the natural flow pattern around the outlets. When adequate pictures had been taken of the trailing edge vortices and Karman sheds,, an angle of attack of 10° to

the freestream was induced on the bluff body via the rotational control rod, and measured by a protractor affixed levelly to the outside of the test section. Once again pictures were taken. The angle was increased until 18°, then decreased to 15 when it became apparent the flow behaved erratically anywhere beyond 15 degrees. When all necessary flow visualization is done with the tab-end plate, the water tunnel was turned off and the water is drain by opening the drain valve. Removing the bluff body and mounting device from the tunnel,, the tab-end plate was separated from the bluff body using a thin box cutter to sever the sealant. The dry sealant on the bluff body and the end plate was removed by slowing rubbing a clean towel against the respected piece. The control endplate was then affixed to the blunt body with sealant and allowed to dry while the water tunnel emptied, the drain closed, and refilled again to 90% capacity. The experiment, beginning from the mounting procedures, was then repeated for this new configuration. At completion of the tests, the water tunnel was shut down and power cut off. The model was removed from the test section and the water tunnel drained. All areas were wiped clean of dye and water, and pictures were uploaded to a computer to review.

IV. Results and Discussion

The dye portals unfortunately did not work as well as hoped for. Even with multiple dye pressurization tubes and separate dye channels for top and bottom portals, it proved impossible to provide enough pressure to get the dye out all six holes without disrupting the flow. Occasional success was observed, but mostly only one or two would work at a time. This potentially could be due to the viscosity or surface tension of the dye, which congealed when left unmoving, and the interaction with the small PVC tubing. While not as effective as hoped for, the system still allowed visualization of the effects a tab induced on the flow properties.

Each test was closely observed and documented via notes, pictures and video. The high quality camera normally used for such procedures unfortunately was disabled at the time, and pictures taken did not always provide enough clarity to see the flows. However, while imperfect, the images captured still demonstrated successful visualization of the bluff body flow characteristics. The difficulty of capturing precise images of the vortexes prompted recording of the tests via the camera's video feature; it captured the rotation of the Karman vortices impressively and provided a useful method to ensure the pictures taken and used in this discussion portrayed an accurate representation of the overall flow conditions seen during each test.

.

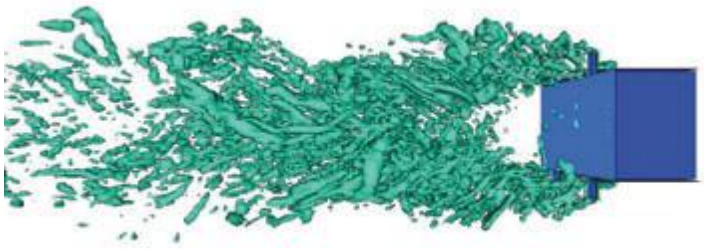

Figure10. This depicts a computerized representation of flow behind a bluff body fitted with tabular passive control[3]

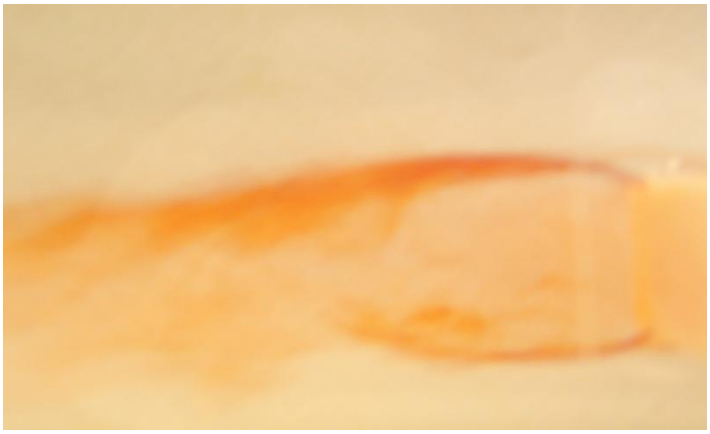

Figure 11. This vortex was observed directly behind the bluff body with tabs, in perfect comparison to the theoretical model shown in Fig. 10

Fig. 10 illustrates a computerized predicted vertical vortex structure behind a tab modified device. Fig. 11 was taken during the tab endplate test of this experiment, when both top and bottom dye portals on the left side of the bluff body were active. This provided first visual confirmation that the model displayed typical and expected flow characteristics, and no aberrations existed in the design to skew results.

This initial proof the tab system was working properly justifies use of the model in verifying the results from the Park experiment. Those findings are stated in this report's introduction, but are reiterated here for ease of reference. Park et.al. found that the tab passive control design would induce the Karman vortex sheds to lose their two dimensional structure and form a three dimensional instead. Previous studies have proven this the main mechanism by which passive control systems reduce drag and pressure disturbances caused by Karman vortex sheds. Park mentioned four main phenomena, that occur due to the tabs, that prove the existence of 3D forcing and drag reduction: suppressed, controlled, and weaker Karman vortices; a longer formation length; formation farther from the trailing edge of the bluff body; and an increase in wake width.

Fig. 12 demonstrates the effectiveness of the passive tab system in suppressing the Karman vortex sheds into steady, small, and controlled cycles.

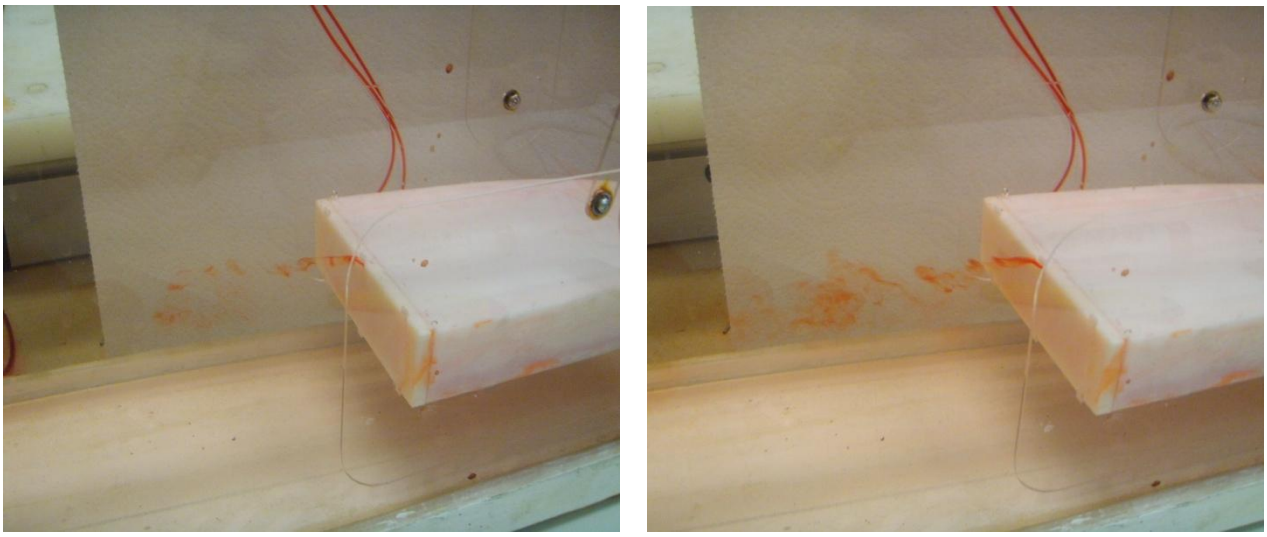

Figure 12. The Karman vortex sheds developed in distinct, separate groups behind the bluff body fitted with the passive control device.

The bluff body model has the tab endplate mounted and rests parallel to freestream flow. As mentioned, only one dye portal was used. However, this one outlet effectively revealed the formation of Karman vortices under influence of the tab device. Note the steady, controlled form of the vortices in the downstream wake and the distinct shape; each vortex is separate from the next, and relatively small in comparison to the body. Fig. 13 below shows the vortex formation without the tab endplate.

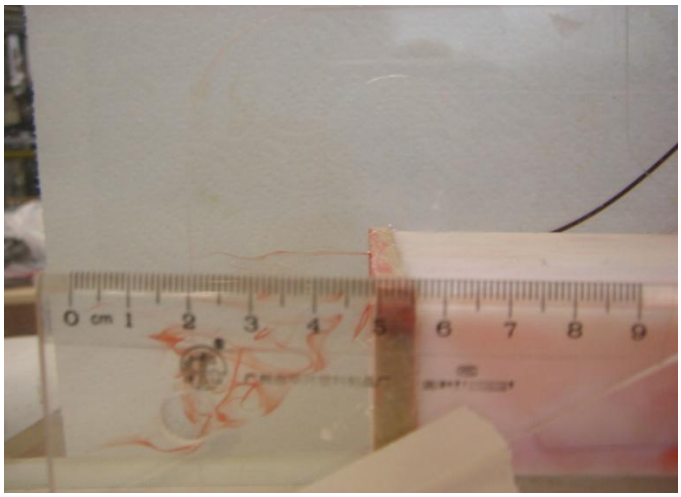

Figure 13. Vortices behind the bluff body with the control endplate affixed displayed more random, strong, and turbulent vortex formation.

Note the existence of large, turbulent, unsteady vortices directly behind the bluff body which is still positioned parallel to freestream flow. The tab device effectively controlled the vortex formation and suppressed the strength. Regular, smaller, and periodically emerging vortices, instead of the erratic and turbulent shapes exhibited by the vortices behind the control case, cause less disturbance in the wake and thus decrease the effects of drag and fluctuations. Fig. 14 shows an additional view of the regular pattern of vortices induced by the tabs.

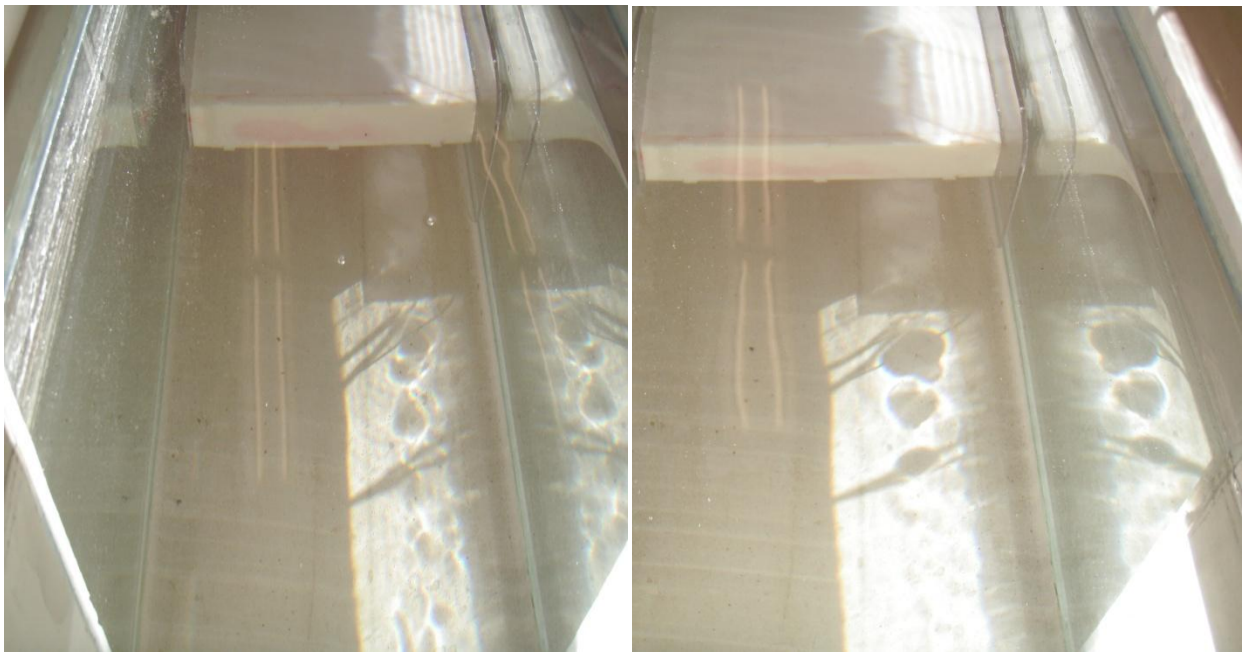

Figure14. Views taken from behind and above the model with the tab endplate before introduction of dye to the system uses light and shadows to illuminate the distinct vortex shapes.

These images were taken before introducing dye into the system, using just the sunlight in the room and shadows. The outline of the vortexes are distinct shapes moving downstream, indicating effective vortex shed control.

Figs. 12, 13 14 also confirm the expected increase in vortex formation length under the influence of the passive control device. Figs. 12 and 14 display longer vortex trails in the wake than the control case displayed in Fig. 13. Such an increase in vortex formation length demonstrates the ability of the tab system to modulate the period of the vortex sheds. Weaker, spread out vortices cause less flow disturbance and thereby less pressure drop in the

immediate rear vicinity of the bluff body, resulting in less of a pressure imbalance between front and back and thus less drag created. Longer vortex formation length thus indicates effective drag control is occurring.

Figs. 15 and 16 show the increased distance from the trailing edge the vortex sheds formed in the control case.

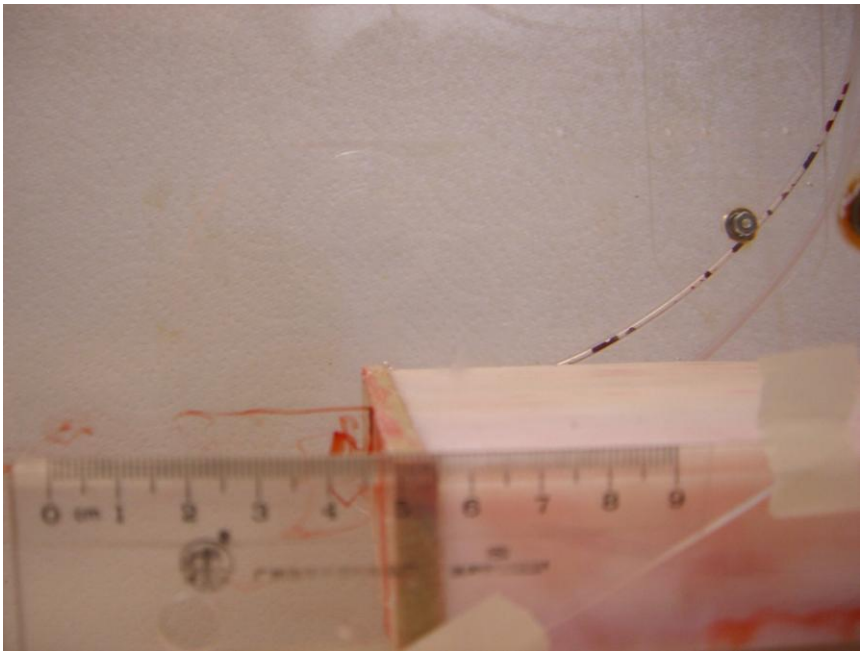

Figure 15. Vortex sheds form close to the trailing edge with no passive control device.

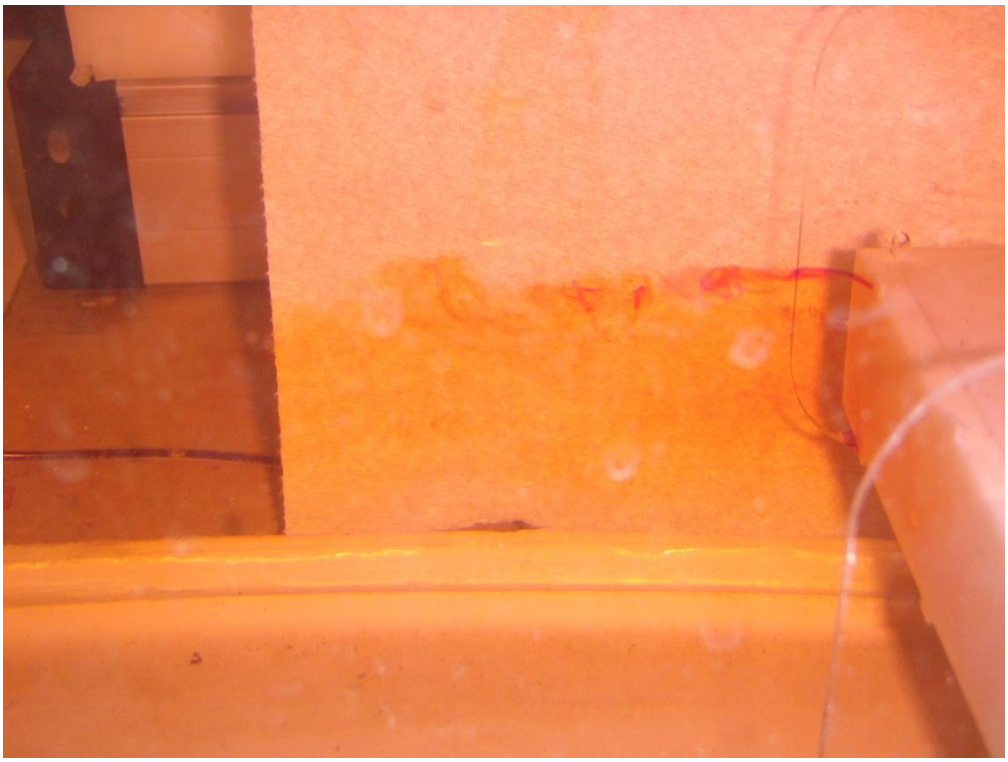

Figure 16. Karman vortex shedding occurs farther from the trailing edge with the passive control system in place.

Fig. 15 depicts the control case; Fig. 16, the tab control system case. Once more the findings of Park et.al are validated. In the tab case the Karman vortex sheds disappear in the immediate vicinity of the trailing edge, and reappear downstream but clearly with less strength than the original vortices illustrated by the no-tab model. The tabs have pushed vortex formation away from the trailing edge. The control case displays a concentration of turbulent vortices at the trailing edge of the bluff body, the usual mechanism that produces large pressure decreases and fluctuations, increasing drag. The ability of the passive tab system to regulate this behavior and spread the vortices to slower frequencies and weaker in strength indicates effectiveness as a drag reduction system, as proposed by Park et.al..attenuated the vortices, further proof of the effectiveness of the tab design. Moving the vortices away from the body reduces their ability to affect the pressure and flow characteristics around the bluff body, thereby reducing the drag induced by the vortex formation.

Thus far, three conditions Park enumerated as evidence of 3D forcing have been visually confirmed. Fig. 17 attempts to capture proof of the fourth, an increase in wake width.

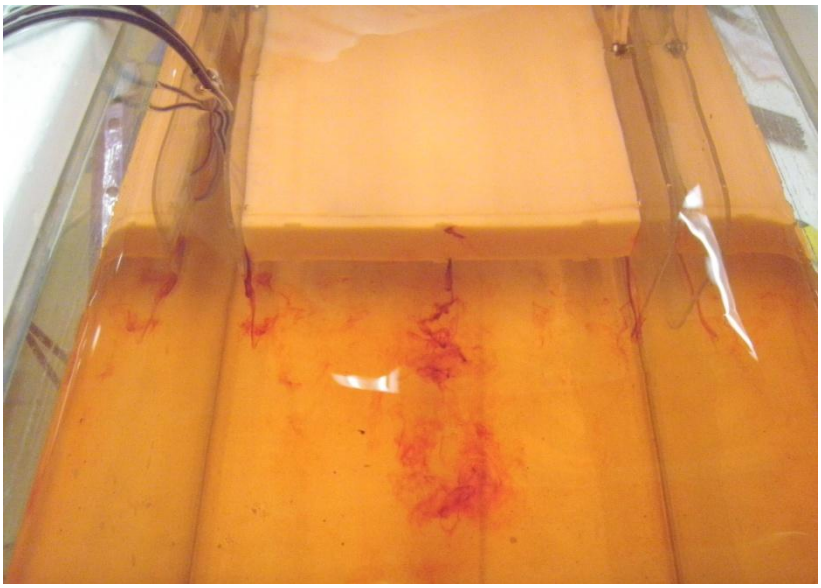

Figure 17. The tab model managed to output dye from all three spanwise locations and depicts the central wake.

Such proof was difficult to obtain due to the failure of the dye control system; without dye ports active on all sides of the model, it was impossible to obtain an image of the entire wake. Fig. 17 was taken during one of the few times dye was successfully dispensed from three ports at once. In comparison to earlier figures of the flow behind, perhaps an increase in wake width can be claimed, but it seems more likely this developed as a result of variations in the amount of dye used. The width may only appear larger because the dye dispensed at different rates between the two cases, or the tab picture may have been taken longer after the dye began dispensing than the control image so the dye may simply have had a longer time to spread out. Without a complete image of the wake the evidence is far from conclusive and highly suspect. Thus this phenomena was not visually observed during this test, but no evidence against its existence was discovered.

Park's experiment was performed only for a bluff body parallel to the freestream flow. Behavior at any angle of attack was not researched in that study. To further experiment with the potential of the design, the flow visualization was performed at a 10 angle of attack, and increased until obvious failure. Fig. 18 displays the bluff body with tab endplate at $\alpha = 10$ in reference to the freestream flow.

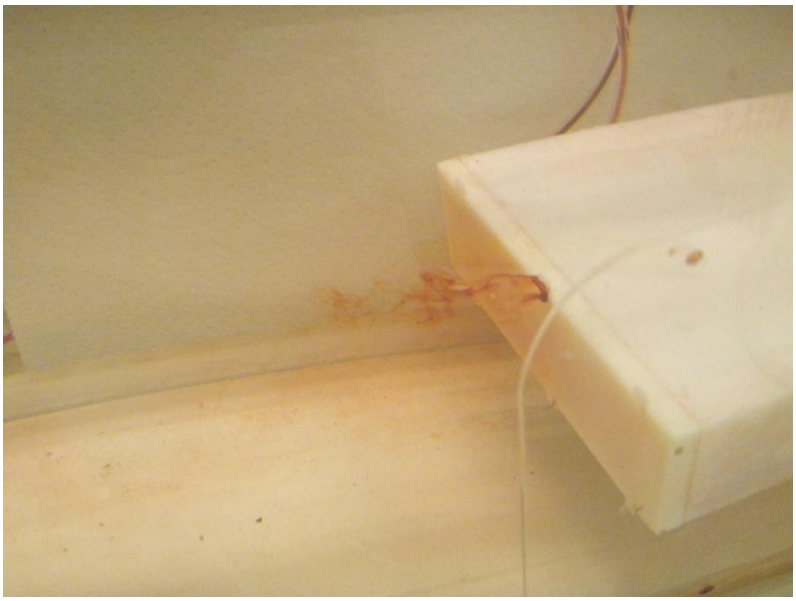

Figure 18. The bluff body with passive control device at α=10 exhibited slightly reduced performance.

A slight deterioration of the system effectiveness is noticeable by the decreased distance between the Karman vortex and the endplate, the reduced length of the vortex sheds, and less well developed vortices. The camera did not quite pick up enough detail to make an obvious statement, but observation did confirm, in comparison to 0 , the α case looked not quite as turbulent as the case with no tabs but certainly moving away from controlled flow. Fig. 19 shows the bluff body with tabs at the highest angle of attack, approximately α = 15 -18 , that could be achieved without total failure of laminar flow and simple boundary layers.

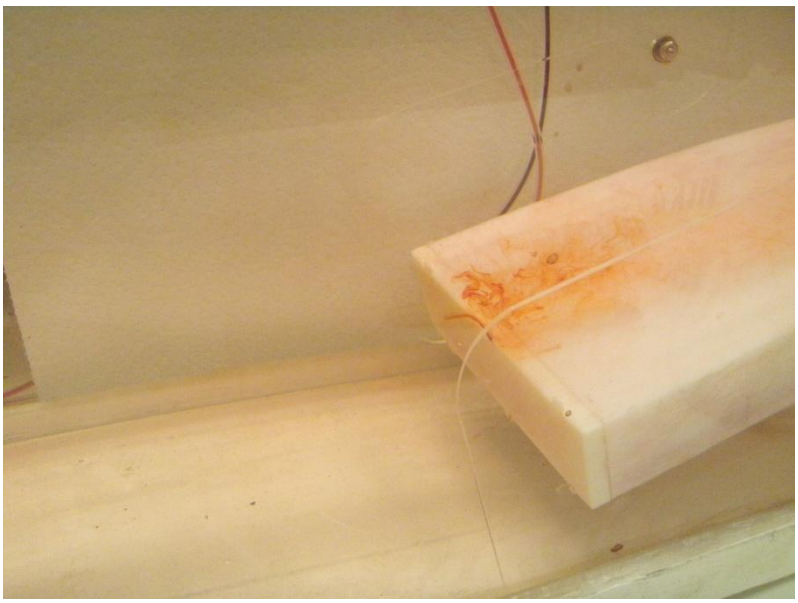

Figure 19. At the highest α experimented, it is clear the tabs do nothing to attenuate the vortex sheds.

Clearly the tabs do not improve performance at high α and their effectiveness rapidly decreases with increasing α. The 15 case exhibits fully turbulent, uncontrolled, and erratic flow typical of that behind angled bodies. Unfortunately only video managed to provide decent photography of the control case for the angle of attack. However, close observation between the video and the image in Fig. 19 revealed little difference between the two; both displayed mass turbulence and vortex production directly behind and directly above the bluff body. This indicates the tabs have no positive effect on the flow at steep values of α.

V. Conclusion

A tabular modification to the trailing edge does indeed disrupt the ordinary flow patterns expected around a bluff body, blunt nose two dimensional structure. The differences noted point out the validity of previous experiments that appointed as the cause the alteration of behavior in the Karman vortex sheds behind the body. Aerodynamicists accept these traits as evidence the vortex characteristics break down into three dimensional form. Use of spanwise modulation, then, appears a viable source for future experimentation on drag and lift fluctuation reduction. However, while the visualization test provided acceptable evidence, improvements to the experiment design could be made to improve accuracy and provide more detailed results. Better imagery mechanisms may capture finer characteristics of the flow unseen by a generic camera and further explain the mechanisms behind the tab system's success. In particular, the flow visualization model did not succeed in fully demonstrating the characteristics of the entire wake due to a flaw in the dye system design. Further improvement to the test model by means of developing a more precise dye control mechanism, distributing dye from all sides of the trailing edge while avoiding any flow disruption, would be advantageous in discovering ways to further the practical application of passive control devices. The lack of precision in this design may have decreased the accuracy of results, particularly during the angled tests. Additional understanding of the flow parameters may lead to invention of a means to keep the device effective at angles to freestream flow, and thus move this passive control device onward from theoretical speculation to the practical world. Experimentation on the effects and possibilities of passive control devices should continue for the potential benefits they could provide to future aircraft, spacecraft, and other engineering innovations.

Acknowledgements

The authors wish to thank Cody Thompson for his machining work on the model, Martin Koch for his assistance with the rapid prototyping machine and advice on manufacturing limitations, and Jin Tso for overseeing and advising this project.

References

[1] Park, H., Lee, D., Jeon, W., Hahn, S., Kim, J., Kim, J., Choi, J., and Choi, H., "Drag Reduction in Flow Over a Two-Dimensional Bluff Body with Blunt Trailing Edge Using a New Passive Device", *Journal of Fluid Mechanics*, Vol. 563, pp 389-414

[2] Anderson, John D. *Fundamentals of Aerodynamics*, 4th Ed., McGraw-Hill, New York, 2007, pp. 239-244, 274-282, 302-319.

[3] Choi, H., Jeon, W., and Kim, J., "Control of Flow Over a Bluff Body", *Annual Review of Fluid Mechanics*, 2008, pp. 113-39